



Association between sagittal alignment and loads at the adjacent segment in the fused spine: a combined clinical and musculoskeletal modeling study of 205 patients with adult spinal deformity

Dominika Ignasiak¹ · Pascal Behm¹ · Anne F. Mannion² · Fabio Galbusera² · Frank Kleinstück³ · Tamás F. Fekete³ · Daniel Haschtmann³ · Dezső Jeszenszky³ · Laura Zimmermann² · Sarah Richner-Wunderlin² · Alba Vila-Casademunt⁴ · Ferran Pellisé⁵ · Ibrahim Obeid⁶ · Javier Pizones⁷ · Francisco J. Sánchez Pérez-Gruoso⁷ · Muhammed Ilkay Karaman⁸ · Ahmet Alanay⁹ · Çağlar Yilgor⁹ · Stephen J. Ferguson¹ · Markus Loibl³ · ESSG European Spine Study Group

Received: 23 March 2022 / Revised: 18 November 2022 / Accepted: 22 November 2022 / Published online: 17 December 2022
© The Author(s) 2022

Abstract

Purpose Sagittal malalignment is a risk factor for mechanical complications after surgery for adult spinal deformity (ASD). Spinal loads, modulated by sagittal alignment, may explain this relationship. The aims of this study were to investigate the relationships between: (1) postoperative changes in loads at the proximal segment and realignment, and (2) absolute postoperative loads and postoperative alignment measures.

Methods A previously validated musculoskeletal model of the whole spine was applied to study a clinical sample of 205 patients with ASD. Based on clinical and radiographic data, pre- and postoperative patient-specific alignments were simulated to predict loads at the proximal segment adjacent to the spinal fusion.

Results Weak-to-moderate associations were found between pre-to-postop changes in lumbar lordosis, LL ($r = -0.23$, $r = -0.43$; $p < 0.001$), global tilt, GT ($r = 0.26$, $r = 0.38$; $p < 0.001$) and the Global Alignment and Proportion score, GAP ($r = 0.26$, $r = 0.37$; $p < 0.001$), and changes in compressive and shear forces at the proximal segment. GAP score parameters, thoracic kyphosis measurements and the slope of upper instrumented vertebra were associated with changes in shear. In patients with T10-pelvis fusion, moderate-to-strong associations were found between postoperative sagittal alignment measures and compressive and shear loads, with GT showing the strongest correlations ($r = 0.75$, $r = 0.73$, $p < 0.001$).

Conclusions Spinal loads were estimated for patient-specific full spinal alignment profiles in a large cohort of patients with ASD pre- and postoperatively. Loads on the proximal segments were greater in association with sagittal malalignment and malorientation of proximal vertebra. Future work should explore whether they provide a causative mechanism explaining the associated risk of proximal junction complications.

Keywords Adult spinal deformity · Spine surgery · Fusion surgery · Sagittal alignment · Musculoskeletal modeling · Adjacent segment · Spinal loads

Introduction

Adult spinal deformity (ASD) is a complex disorder associated with decreased health-related quality of life [1]. The prevalence of ASD is estimated to be between 32 and 68%

in individuals over 65 years of age [2]. With the growing proportion of older individuals in the global population, the associated socioeconomic costs will continue to rise [3]. Due to degenerative processes, ASD typically involves pathological changes in the sagittal plane (sagittal imbalance, spondylolisthesis) and frontal and transverse plane (i.e., scoliosis). Surgical correction of spinal deformity can relieve pain and reduce disability, with outcomes that seem superior to

✉ Dominika Ignasiak
dominika.ignasiak@hest.ethz.ch

Extended author information available on the last page of the article

those of conservative treatment in selected patients [4, 5], but complications are not uncommon [6].

Mechanical complications caused by continuous or repetitive mechanical stress are estimated to affect 28–61% of ASD patients with longer fusion constructs (≥ 4 spinal levels) [7, 8]. They include proximal junctional kyphosis (PJK) or failure (PJF), distal junctional failure, pseudoarthrosis, rod breakage, screw pull-out and other implant-related complications [9, 10]. These complications lead to revision surgery in 12–35% of all cases [11, 12]. The factors contributing to the risk of complications: older age, osteopenia, presence of comorbidities, higher BMI, and large abnormalities in preoperative sagittal alignment [13, 14], affect body biology, biomechanics, or both.

Spinal sagittal malalignment has been identified as an important biomechanical factor affecting both the risk of mechanical complications [15–17] and patient self-reported outcome [18–20]. Restoration of normal sagittal alignment is therefore one of the critical aims of adult spinal deformity surgery [4, 15]. Based on the clinical observations, it has been proposed that postoperative alignment can predict future mechanical complications. For example, the recently developed Global Alignment and Proportion (GAP) score—a scoring system for postoperative spinal sagittal shape and alignment relative to patient-specific pelvic incidence [9]—has been shown promising accuracy in predicting mechanical complications after ASD surgery [8, 9, 21–24]. From a biomechanical perspective, severe malalignment is expected to be related to unfavorably large spinal loads, contributing to the risk of mechanical failure. However, considering the complexity and variability of the spine curvature, the relationships between global sagittal alignment and spinal loads are not trivial.

Previous biomechanical modeling works exploring these relationships [25–27] revealed that even small changes in thoracic [27] or lumbar [26] curvature can have substantial impact on spinal loads. In sagittally malaligned postures, trunk center of mass is generally shifted anteriorly, which requires higher extensor muscle forces, resulting in elevated spinal loads. Consequently, loads increase with more pronounced thoracic kyphosis [28, 29], and are mitigated by congruent lumbar lordosis [29, 30] and—to some extent—by compensatory mechanisms such as pelvic retroversion [29]. In other words, not only segmental and regional alignment affect spinal loads, but also their interplay, i.e., global sagittal alignment, matters. A recent simulation study of 2772 synthetically created normal spino-pelvic alignment profiles found that spinal loads were modulated by the combined effects of global alignment (reflected by SVA, sagittal vertical axis), lumbar topology (Roussouly types [31]) and sacral inclination [32]. The relationships between global and local alignment and spinal loads have not been yet explored in-depth in a surgical patient population. Previous studies

investigating postoperative loads considered the lumbar spine only and were focused on short (L4-L5 and L4-S1) fusions [33, 34], disregarding the effects of thoracic curvature and longer fusion constructs.

Therefore, the main aim of this combined clinical and computational study was to investigate pre- and postoperative spinal loads at the proximal segment in patients with ASD in relation to their sagittal alignment profiles, using patient-specific musculoskeletal modeling and radiographic data.

1. We aimed to investigate the association between surgical realignment of the vertebral profile (pre-to-postop change in sagittal alignment measures) and the corresponding change in loading at the segment adjacent to the spinal fusion. We hypothesized that a greater realignment would be associated with a greater reduction in compressive load and a greater negative change in shear force (i.e., more posterior shearing).
2. A second aim was to explore the association between postoperative global sagittal alignment and absolute postoperative spinal segmental loads. Our hypothesis was that greater measures of malalignment would be associated with greater loads at the proximal adjacent segment, which might be indicative of a potential mechanical failure mechanism.

To test these hypotheses, a previously established and validated musculoskeletal model of the spine with fusion effects was used [35, 36]. Retrospective review of prospectively collected radiographic and demographic data of patients with ASD served to construct patient-specific preoperative and postoperative models allowing simulation of related spinal loads at the proximal segment.

Methods

Patient dataset

A retrospective dataset of 222 patients with ASD was used, the same cohort described in the previous clinical study in which the Global Alignment and Proportion (GAP) score was developed and validated [9]. The data were collected within the multicenter study of the European Spine Study Group (ESSG), a collaboration of 6 clinical sites across Europe. Enrollment criteria were: age of ≥ 18 years and at least 1 of the following: coronal Cobb angle $\geq 20^\circ$, sagittal vertical axis of ≥ 5 cm, pelvic tilt of $\geq 25^\circ$, or thoracic kyphosis of $\geq 60^\circ$. Out of this ESSG database, only cases of operative treatment with posterior fusion at ≥ 4 levels and follow-up data available at ≥ 2 years postoperatively were included in the GAP study [9] and in the current work. Further exclusion criteria, related to the simulation nature of the

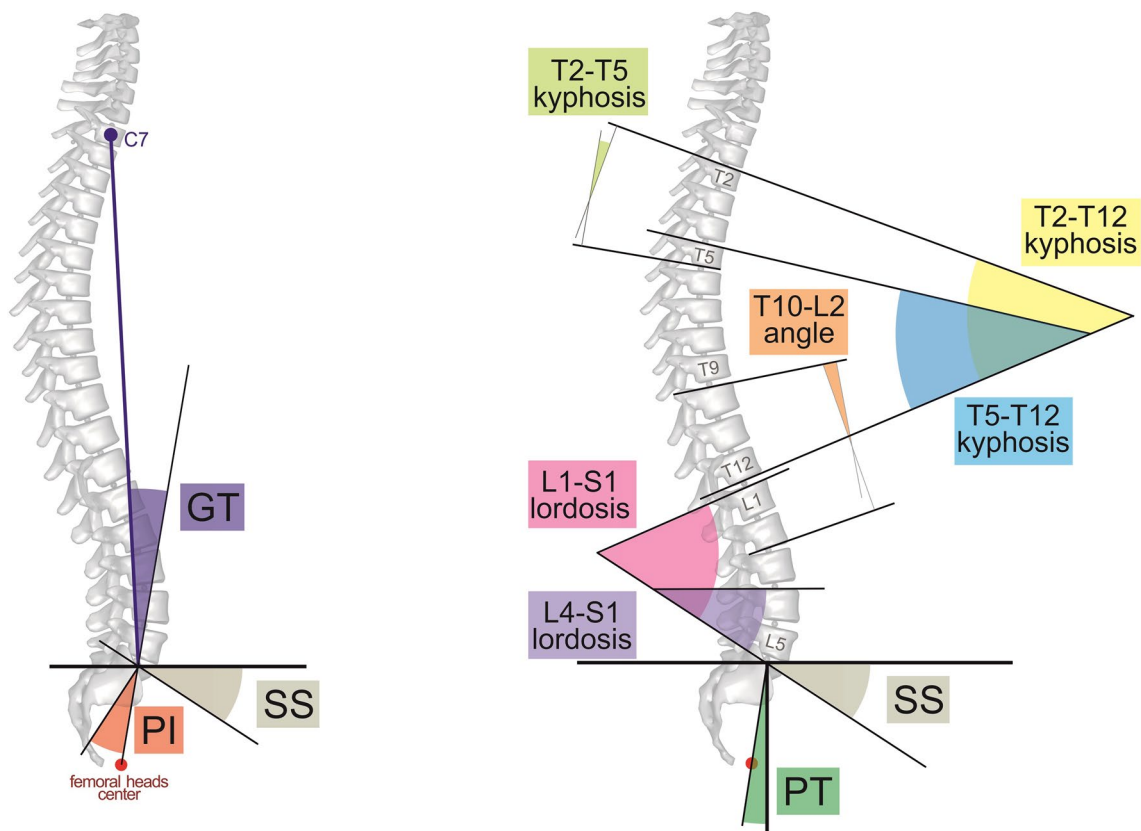


Fig. 1 Spino-pelvic parameters obtained from pre- and postoperative radiographs for constructing subject-specific models of sagittal alignment profiles (SS-sacral slope, PI-pelvic incidence, PT-pelvic tilt, GT-global tilt)

study were: upper instrumented level at T1 or more superior (unsuitable to be simulated with the model established for investigating loads at T1/T2-L5/S1), missing values of postural measures needed to create a patient posture model within the defined work frame, or model construction and simulation errors.

The dataset included patient demographic parameters, surgical treatment details, prior fusion, occurrence and type of mechanical complications, as well as sagittal alignment measures obtained from preoperative and 6 weeks postoperative long lateral radiographs. The sagittal alignment parameters included: pelvic incidence (PI), sacral slope (SS), global tilt (GT), lumbar lordosis L1-S1 and thoracic kyphosis T2-T12 angles, and angles for estimating lumbar and thoracic curve distribution: L4-S1, T10-L2, T5-T12, and T2-T5 (Fig. 1). Based on the sagittal parameters, GAP score and its parameters (relative pelvic version, RPV; relative lumbar lordosis, RLL; lordosis distribution index, LDI; and relative spinopelvic alignment, RSA) were calculated for each participant (Fig. 2). GAP score can be used to categorize sagittal alignment as: postoperatively proportioned, $GAP \leq 2$; moderately disproportioned, $3 \leq GAP \leq 6$; and severely disproportioned, $GAP \geq 7$ [9].

The spine model

A musculoskeletal model of the spine, including articulated thorax with ribcage, previously developed and validated in the AnyBody Modeling System software was used [35, 36]. In this model, the pelvis is constrained to the ground and rigidly connected to the sacrum. The articulations between thoracic and lumbar vertebrae are modeled as spherical joints, and articulations between ribs and vertebrae are approximated as revolute joints. The elastic effects of intervertebral disc, paraspinal ligaments and ribcage structures are modeled with passive stiffness elements. This model has been validated by comparing predicted compressive forces to reported *in vivo* intradiscal pressure measurements at various postures in healthy volunteers, as described in more detail in previous works [35–38]. The previously established model extension was used for modeling the effects of spinal fusion [39]. In this model, the surgically treated levels are selected as the model input, and fused vertebrae are modeled as rigidly connected, i.e., not allowing any motion at fused joints and fully transferring forces and moments.

Fig. 2 Summary of the GAP scoring system of the sagittal alignment (based on [9]). Based on the cut-off values (not shown), the parameter measures (RPV, RLL, LDI, RSA) are scored for severity of malalignment. The GAP score reflects the sum of these partial scores

RPV	Relative Pelvic Version RPV = Measured - Ideal Sacral Slope Ideal Sacral Slope = Pelvic Incidence x 0.59 + 9	Anteversión	1
		Aligned	0
		Moderate retroversion	2
		Severe retroversion	3
RLL	Relative Lumbar Lordosis RLL = Measured - Ideal Lumbar Lordosis Ideal Lumbar Lordosis = Pelvic Incidence x 0.62 + 29	Hyperlordosis	3
		Aligned	0
		Moderate hypolordosis	2
		Severe hypolordosis	3
LDI	Lordosis Distribution Index LDI = $\frac{\text{L4-S1 Lordosis}}{\text{L1-S1 Lordosis}} \times 100\%$	Hyperlordotic maldistribution	3
		Aligned	0
		Moderate hypolordotic maldistribution	1
		Severe hypolordotic maldistribution	2
RSA	Relative Spinopelvic Alignment RSA = Measured - Ideal Global Tilt Ideal Global Tilt = Pelvic Incidence x 0.48 - 15	Negative malalignment	1
		Aligned	0
		Moderate positive malalignment	1
		Severe positive malalignment	3
Age Factor		Adult (<60 y. o.)	0
		Elderly Adult (≥60 y.o.)	1

GAP score = 0 - 13

Patient-specific models

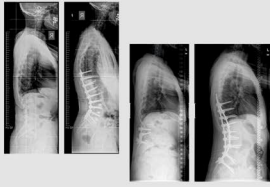
Patient-specific sagittal spinopelvic alignment profiles were represented in the musculoskeletal spine model (Fig. 3), taking into account the aforementioned radiographic parameters. The orientation of sacrum was set according to the measured SS angle. Pelvis rotation with respect to sacrum was set to represent individual PI. The measures of L4-S1, L1-S1, T10-L2, T2-T12, T5-T12 and GT angles were used to set relative orientations of associated vertebrae in the sagittal plane. The curvatures defined by these measures were distributed equally between the intervertebral joints encompassed by a measure (e.g., L4-S1 angle was divided into equal angles of L4-L5 and L5-S1). Horizontal gaze was assumed, by setting skull orientation and allowing cervical spine to flex/extend so such position of the head is achieved. Endplate slope of the upper instrumented vertebra, UIV_slope, was estimated in the reconstructed alignment model, measured as an angle between the upper endplate of UIV and the horizontal line. Patient models were scaled uniformly to represent individual body weight and height. In this way, pre-and postoperative models were constructed. Fusion effects were modeled for the surgically treated segments. In revision surgery cases, prior fusion was modeled in the preoperative model.

Simulations

Inverse-static simulations of pre-and postoperative patient-specific models of sagittal alignment were performed in the AnyBody Modeling System [40]. In the simulation, internal forces (muscle and joint reaction forces) needed to support the modeled posture were computed [41]. Because of muscle redundancy in the system, a muscle optimization scheme was applied to mimic physiological recruitment of the muscles by the central nervous system, favoring stronger muscles and muscle synergy [42]. The muscle recruitment criterion used was a sum of cubed muscle activities (activity is defined as a ratio of generated muscle force to its strength, or maximum force it can generate). Compressive and antero-posterior shear forces were calculated (Fig. 4) for all the unfused spinal segments. Loads analysis was performed for the segment proximal to the instrumentation (with estimation of loads at the center of intervertebral disc proximal to the UIV) in the postoperative condition and for the corresponding segment in the simulated preoperative condition, to analyze pre-to-postop changes in loading conditions of the proximal segment. To allow between-subjects comparability, the loads were normalized to individual body mass.

Retrospective Chart Review

ASD patients, N = 205
long fusion (4+ levels)



Radiographic & Clinical Data

- Spinopelvic sagittal alignment parameters (PI, SS, L1-S1 & L4-S1 lordoses, T2-T12, T5-T12, T2-T5 kyphoses, T10-L2 angle, GT)
- Body weight
- Body height
- Fused levels

Patient-specific Musculoskeletal Models

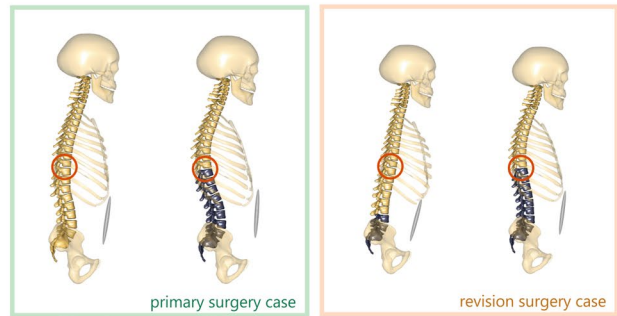


Fig. 3 The overview of the study design: radiographic and clinical data was used to construct individualized spine models reflecting pre- and postoperative conditions. Inverse-static simulations were per-

formed to estimate compressive and antero-posterior shear loads at the segment adjacent to fusion and at the corresponding spinal level preoperatively

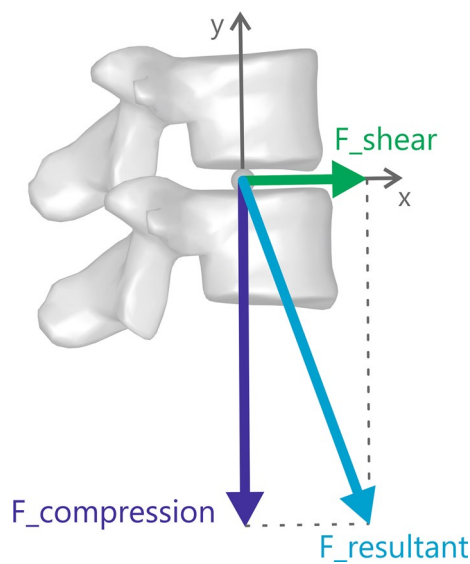


Fig. 4 As a result of the simulation, spinal segmental loads ($F_{resultant}$) are found as intervertebral joint forces for each unfused spinal segment. Axial compression and antero-posterior shear components are calculated with respect to the reference frame of the intervertebral disc space. (Estimation of proximal segment loads at the center of the intervertebral disc proximal to the upper instrumented vertebra)

was set at $p < 0.05$, and the Benjamini–Hochberg procedure was applied to adjust p -values for multiple hypothesis testing and control the false discovery rate at the 5% level. Analyses were performed using MATLAB (MATLAB R2018a, v. 9.4.0, MathWorks, Inc.).

Results

Patient sample

Out of the sample of 222 patients, 17 were excluded. Eight had an upper instrumented level at T1 or more superior. In five cases, the dataset of postural measures was incomplete. In four other cases, data were available, but posture could not be simulated (due to model limitations: assumed dimensions of vertebral bodies and intervertebral spaces causing conflict between provided sagittal alignment measures, or simulation failure to solve extreme deformity cases). This left $N = 205$ patients (156 female, 49 male) to be analyzed in the study. Their mean age (and standard deviation) was 52.1 ± 19.2 years (range 18–84 years), mean body mass 67.5 ± 13.6 kg (range 40–110 kg), body height 162 ± 9 cm (range, 143–192 cm), BMI 25.7 ± 5.1 kg/m² (range, 13.4–44.6 kg/m²).

The sample included both primary (72%) and revision (28%) surgery cases, representing a variety of fusion lengths (median number of fused motion segments = 9, range 3–16), and upper (T2–L3) and lower (T12–pelvis) instrumented levels, with T10–pelvis fusion being the most common (13%, Fig. 5). All considered sagittal alignment parameters showed significant changes from preoperative to postoperative (Table 1). The sample covered a range of sagittal deformity severities: classifying according to the GAP score categories, 35% cases showed postoperatively

Statistical analyses

Descriptive data are presented as means \pm standard deviations (SD). Wilcoxon signed-rank tests were performed to examine differences between preop and postop measures. Postoperative changes in model-predicted compressive and shear forces estimated for the proximal segment (with respect to the corresponding segment in the preoperative condition) were calculated. Their associations with sagittal alignment measures and the associations between sagittal alignment measures and spinal loads were analyzed with Pearson’s r correlation coefficients. The significance level

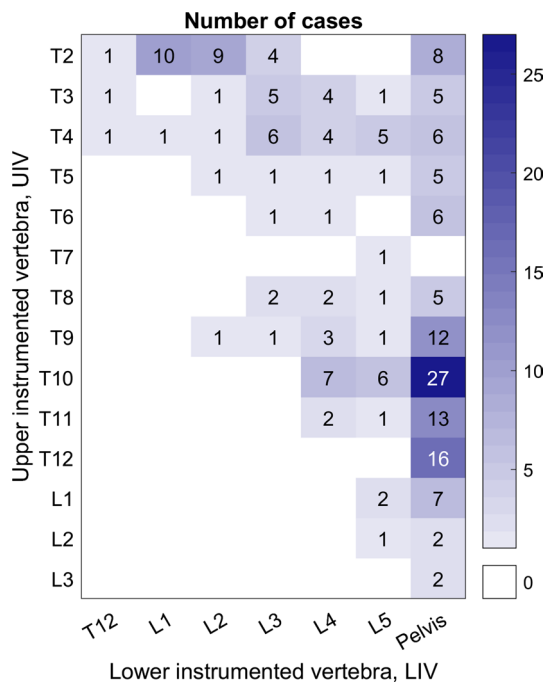


Fig. 5 Number of cases with fusion at a given upper (y-axis) and lower (x-axis) instrumented vertebra

proportioned sagittal alignment ($GAP \leq 2$), 37% moderately disproportioned ($3 \leq GAP \leq 6$), and 28% severely disproportioned ($GAP \geq 7$).

Relationship between realignment and postoperative change in segmental load

Significant weak-to-moderate correlations (Pearson’s r range: 0.17–0.44 and -0.20 to -0.43) were found between pre-to-postop changes in some of the alignment measures and changes in the predicted body-mass-normalized compressive ($\Delta Compr/BM$) and shear loads ($\Delta Shear/BM$) at the proximal segment (Table 2). In particular, the ΔLL (hence also ΔRLL), ΔGT (ΔRSA) and ΔGAP score correlated with both compressive and shear loads. Changes in: GAP score and all of its parameters (ΔRPV , ΔRLL , ΔLDI , ΔRSA), thoracic angles ($\Delta T2-T12$, $\Delta T5-T12$) and in the endplate slope of the upper instrumented vertebra (ΔUIV_slope) were associated with changes in shear force at the proximal segment. A case illustrating these associations is presented in the Fig. 6.

Postoperative alignment and loads at the proximal segment

The relationships between the spinal loads at the proximal segment and postoperative sagittal alignment were analyzed for T10-pelvis fusion cases ($N=27$). Spinal loads depend on fusion location [39], and T10-pelvis fusion was the most numerous patient subgroup with 27 individuals (Fig. 5). Significant moderate and strong correlations were found between postoperative compression and shear forces (normalized to body mass) at the proximal T9–T10 segment and several alignment measures (GAP, RSA, GT, PI-LL mismatch, PT, T10-L2, UIV_slope) (Table 3), with global tilt

Table 1 Pre-and postoperative radiographic parameters in the analyzed patient sample. Significant differences ($p < 0.05$), as determined by Wilcoxon signed-rank test, are highlighted with a bold font

	Preop		Postop		<i>p</i> -value
	Mean	SD	Mean	SD	
PI	54.2	12.9			
SS	30.9	12.6	33.4	10.2	< .001
PT	23.2	12.3	20.8	10.3	< .001
LL	42.6	22.2	52.0	14.4	< .001
PI-LL	11.6	22.8	2.1	14.3	< .001
L4-S1	34.7	15.1	32.7	9.3	0.038
T2-T12	37.3	19.4	42.8	14.3	< .001
T5-T12	31.2	19.1	34.1	13.1	0.003
T2-T5	9.2	8.7	11.0	7.5	< .002
T10-L2	12.9	17.3	5.8	11.9	< .001
GT	26.5	17.9	21.3	13.2	< .001
GAP	7.2	4.4	4.3	3.6	< .001

PI—pelvic incidence; SS—sacral slope; PT—pelvic tilt (derived as PI-SS); LL—lumbar lordosis (L1-S1); PI-LL—pelvic incidence—lumbar lordosis mismatch; L4S1—lower lumbar lordosis; T2-T12, T5-T12, T2-T5—thoracic kyphoses angles; T10-L2—thoracolumbar junctional angle; GT—global tilt; GAP—GAP score

Table 2 Univariate correlations between pre-to-postop changes in loads at the proximal segment and changes in sagittal alignment parameters, including GAP score and its parameters (RPV, RLL, LDI, GT), thoracic angles and endplate slope of UIV (with respect to horizontal line)

	Δ Compr (/BM)		Δ Shear (/BM)	
	Pearson's r	p-value	Pearson's r	p-value
Δ GAP	0.26	<0.001	0.37	<0.001
Δ SS (Δ RPV)	-0.08	0.248	-0.20	0.005
Δ LL (Δ RLL)	-0.23	<0.001	-0.43	<0.001
Δ LDI	0.13	0.054	0.17	0.012
Δ GT (Δ RSA)	0.26	<0.001	0.38	<0.001
Δ T2-T12	-0.13	0.058	-0.40	<0.001
Δ T5-T12	-0.09	0.176	-0.33	<0.001
Δ T2-T5	0.01	0.857	0.05	0.519
Δ T10-L2	-0.13	0.061	-0.03	0.685
Δ UIV_slope	0.17	0.014	0.44	<0.001

(Note that RPV depends on the ratio of patient's SS to PI, so its postop-preop change is de facto Δ SS, assuming PI is unchanged after surgery. Following similar logic, also Δ RLL \approx Δ LL, and Δ RSA \approx Δ GT). Significant correlations (corrected p-value < 0.0139, found by controlling the false discovery rate at 5% level in multiple hypotheses testing using Benjamini–Hochberg method) are highlighted with a bold font

(and consequently RSA, measure based on GT) showing the strongest associations with loads (Fig. 7).

Discussion

Mechanical complications after adult spinal deformity surgery remain a problem affecting patient outcomes. Spinal sagittal alignment has been recognized as a risk factor, and has been proposed as a predictor of mechanical complications risk, e.g., by a scoring system of Global Alignment and Proportion (GAP). The aim of the current study was to explore the possible underlying biomechanical causes related to sagittal malalignment leading to mechanical complications through the analysis of model-predicted loads at the proximal segment in relation to postoperative alignment and the extent of surgical realignment. Loads acting on the spine after spinal fusion surgery may negatively affect proximal segment. Excessive compressive loads may cause vertebral body fractures [43, 44], while shear overload may lead to facet joint injuries and pedicle fractures [45] or contribute to screw pull-out.

Changes in alignment from preoperative to postoperative found in this study were weakly-to-moderately associated with changes in loads, and moderate correlations were found between postoperative alignment and postoperative loads in T10-pelvis fusion cases. These results suggest that biomechanical loads are influenced by postoperative changes in alignment, in particular global balance, and likely contribute to the risk of developing mechanical complications. Their

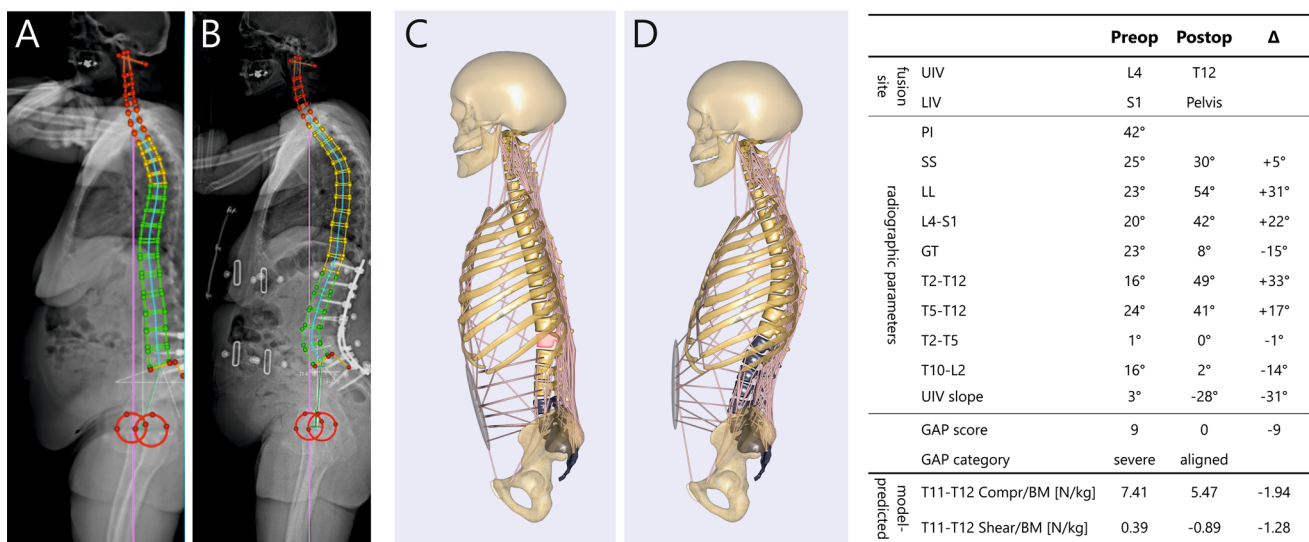


Fig. 6 An example patient case illustrating the associations between the change in alignment and change in loads at the adjacent segment. Sagittal alignment measures (listed in the table) were obtained from the annotated radiographs (A, B) and served to construct patient preoperative C and postoperative D models. Loads calculated at the T11-T12 intervertebral disc space proximal to the T12-Pelvis fusion (fusion shaded in gray) in the postoperative model and at the same level preoperatively (T12 vertebra marked for reference in pink in the

figure C) are presented in the table. In this patient case, the surgery resulted in markedly improved alignment, as reflected in the restored LL and decreased GT and GAP score. The compressive load at the adjacent segment (T11-T12) predicted by the musculoskeletal model was 26% lower than the preoperative load at this level. Model-predicted shear changed direction from anterior to posterior and doubled in magnitude

Table 3 Univariate correlations between postoperative loads (normalized to BM) at the T9T10 proximal segment and sagittal alignment parameters

	Compr (/BM)		Shear (/BM)	
	Pearson's r	p-value	Pearson's r	p-value
GAP	0.51	0.007	0.51	0.007
RPV	-0.20	0.319	-0.27	0.169
RLL	-0.38	0.049	-0.29	0.135
RSA	0.69	<0.001	0.62	<0.001
LDI	0.26	0.186	-0.04	0.846
GT	0.75	<0.001	0.73	<0.001
PI-LL	0.51	0.007	0.44	0.021
LL	-0.17	0.404	-0.06	0.752
SS	0.07	0.719	0.07	0.716
PT	0.41	0.031	0.56	0.003
L4-S1	-0.19	0.351	-0.18	0.378
T2-T12	0.31	0.115	0.20	0.313
T2-T5	-0.13	0.516	-0.29	0.136
T5-T12	0.34	0.083	0.26	0.191
T10-L2	0.58	0.002	0.53	0.004
UIV_slope	0.67	<0.001	0.48	0.012

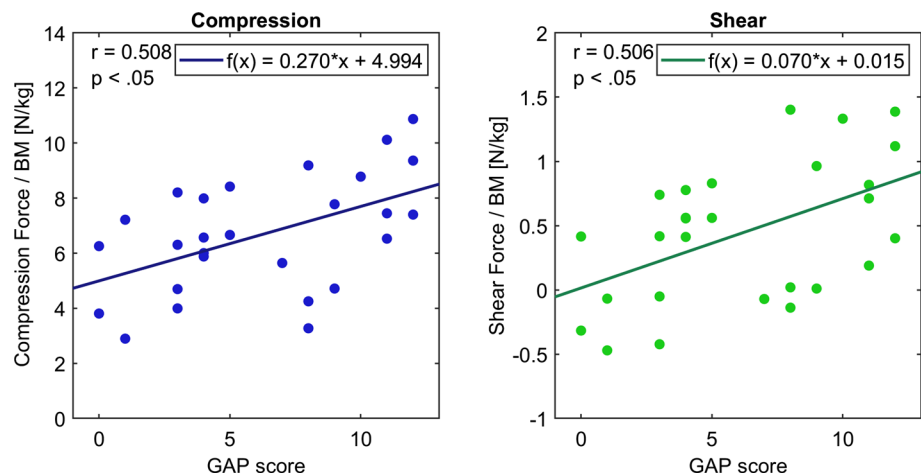
Significant correlations (corrected p -value < 0.0123 , found by controlling the false discovery rate at 5% level in multiple hypotheses testing using Benjamini–Hochberg method) are highlighted with a bold font

exact role, which could explain the relationship between sagittal alignment measures (such as GAP score), and the risk of proximal junction complications should be further evaluated in future studies.

The relationship between postoperative loads and sagittal alignment has been explored in previous modeling studies focused on short (1 or 2 levels) lumbar fusions [33, 34]. Shear loads at the segment adjacent to L4–L5 fusion were found to be markedly affected by the alignment change due

to fusion, with increased shearing predicted for hypolordotic fusion angles and decreased shear for hyperlordotic (with respect to preoperative angle). The negative correlation found in the current study between pre-to-postop change in lumbar lordosis angle and change in shear at the adjacent segment ($r = -0.43$, Table 2) indicates a similar relationship in long spinal fusion constructs (≥ 4 spinal levels). Although here the adjacent segment is more distant from the lumbar region, the amount of lordosis influences the antero-posterior position of the trunk center of mass and the inclination of the adjacent segment, affecting in turn flexion moments to be balanced by the muscles, and therefore the predicted loads.

By modeling full spinal sagittal profiles, this work investigated how the adjacent segment loading conditions are impacted not only by local or regional but also global measures of sagittal alignment. The postoperative improvement in GAP score was found to be weakly and moderately associated with the changes in compression and shear loads, respectively, and the change in relative lumbar lordosis ($\Delta RLL \approx \Delta LL$) and relative spinopelvic alignment ($\Delta RSA \approx \Delta GT$) seemed to be the GAP score parameters influencing this relationship the most. The change in lumbar curvature distribution (ΔLDI) and change in relative pelvic version ($\Delta RPV \approx \Delta SS$) were correlated with the postoperative change in loads only weakly ($r < 0.2$) or not at all. Postoperative changes in shear seemed to be associated also with changes in global (T2-T12) and lower (T5-T12) thoracic kyphosis angles. Some studies have found increased postoperative thoracic kyphosis to be associated with [46] and predictive of the development of PJK [47]. Our results indicated as well that realignment resulting in a pronounced change in the UIV endplate slope (in either direction) might cause an unfavorable change in loading conditions at the proximal segment. A corresponding large change in shear likely affects load vector direction and may initiate fracture in the vertebrae, as trabecular structure is more vulnerable

Fig. 7 Body-mass normalized compressive (left) and antero-posterior shear (right) forces at proximal segment T9-T10 predicted by the simulations of the T10-pelvis fusion cases ($N=27$)

under off-axis loads [48]. The orientation of the UIV segment postoperatively has been the subject of clinical consideration as a risk factor for PJK [49], but the relative change with respect to preoperative alignment and its role in complication risk have not been assessed.

In the analysis of adjacent segment loads in the subgroup of T10-pelvis fusion cases, global sagittal alignment measures, i.e., GT and GAP, correlated moderately to strongly with compressive ($r=0.75$, and 0.51 , respectively) and shear ($r=0.73$ and 0.51) forces (Table 3, Fig. 7). While strong associations were found between the adjacent segment forces and global tilt (hence derived RSA, GAP parameter), no significant correlations were found with RPV, RLL or LDI (i.e., other GAP parameters). It is possible that these GAP parameters are of higher relevance for loads in fusion cases other than T10-pelvis fusions considered here, as the GAP scoring system was developed as a more universal tool evaluated for use with a wider variety of surgical cases. The imbalance in respective relevance of GAP measures might explain the discrepancies between the studies evaluating GAP score validity in different patient cohorts with various sagittal profile characteristics (e.g., [9–12, 21, 24]).

Study limitations

1. Absolute loads (rather than changes in loads) analysis was carried out only for the T9-T10 segment being the adjacent segment to T10-pelvis fusion, possibly limiting generalizability of the conclusions. On the other hand, T10-pelvis represents one of the most common selection of fusion levels.
2. Changes in loads were analyzed collectively for various adjacent segment levels, although they might be influenced by the spinal level, as well as the extent and location of fusion. (For example, it is possible that postoperative change in compressive loads might be greater for cases with more caudal UIV, since caudal segments generally carry greater loads to begin with.)
3. Only forces at the proximal segment were analyzed, allowing interpretation of the results in the context of PJK or PJF risk only. This needs to be noted particularly when interpreting relationships to GAP score, which was designed to predict other mechanical complications as well (distal segment problems and implant-related complications) that are likely unrelated to loads at the proximal segment.
4. Reconstruction of patient posture in the spine model was based on several global and regional measures obtained from radiographs, but the intervertebral angles were only estimated, assuming even distribution of the curvature among constituting segments. This might have led to inaccuracies in representing the true patient-specific vertebral alignments (e.g., note more even distribution of kyphosis in the model compared to the radiographs in the example case presented in the Fig. 6), although it remains questionable whether this would have a large impact on the prediction of spinal loads. The inaccuracy in vertebral orientation might influence the predicted load direction (i.e., shear component relative to compression), but the overall biomechanics and predicted load magnitudes are not expected to be greatly influenced (thoracic and global measures were taken into account, which should provide a good approximation of the gravity moments in the model).
5. The study focused solely on mechanical loads related to sagittal alignment, as possible risk factors for postoperative mechanical complications, disregarding likely contribution of other factors. Mechanical failure occurs when the tissue and / or implant strength is not sufficient to withstand loads acting on it. A variety of biological, mechanical and surgical factors affects this relationship and can result in a catastrophic failure. For example, low bone mineral density [50, 51] smoking and comorbidities reported to affect the complication risk [52] are likely related to compromised tissue health and ability to sustain load. Such factors have not been considered in this work (nor are they accounted for in the GAP score).
6. Beside sagittal alignment, body weight and height, no other patient-specific characteristics were included in the musculoskeletal model. Body weight and height are relevant, as BMI has been found to be related to adjacent segment degeneration [53] and complications [52]. However, disregarding the effects on spinal loads of patient-specific properties of muscles (including their maximum force generating capacity) and ligaments as well as intervertebral disc degeneration constitutes a limitation. In particular, the role of the musculature in the maintenance of sagittal alignment [54, 55] and proximal segment pathology has been reported [51, 55], and muscle health affects spinal loads in a degenerated [56] or surgically treated [57] spine.
7. The analyses were performed only for static upright posture. It is possible that some postural traits have implications for movement and transfer of forces during dynamic activities (beyond the scope of this study) that can contribute to mechanical complications. Future modeling work should be performed to simulate various sagittal alignment types during dynamic motion tasks.
8. The musculoskeletal model used was previously validated in terms of predicted loads at selected body postures and spinal levels in healthy subjects only [35, 36]. Further validation remains extremely challenging due to the limited data available and invasiveness of the measurements required. However, the validation works performed to date have shown correct trends in the

predicted loads, indicating that the model components interact with each other in the expected manner, which supports the assumption of model suitability to analyze other conditions.

Extending the analysis to a larger clinical cohort and including factors other than alignment (especially measures of frailty, indicative of tissue health) and simulating motion tasks could allow quantification of the relative role that sagittal alignment plays via modulation of spinal loads in developing complications. More generally, the analysis of spinal loads could help to elucidate potential mechanisms explaining the progression of spine degeneration, with spine shape as a mechanical factor [58]. Nevertheless, this study highlights the importance of considering the sagittal alignment in the treatment of spinal disorders [59]. It also demonstrates the value of musculoskeletal modeling in investigating the complex biomechanics of spinal sagittal alignment, which is highly variable between individuals [31] and influenced by pathological and compensatory changes [58, 60].

Conclusion

To the authors' knowledge, this is the first study of spinal loads estimated for real patient-specific spinal alignment profiles in a large ASD patient cohort pre- and postoperatively. The results indicate that global and local alignment measures, interconnected through spine congruency and geometrical relationships, influence the loads on the proximal segment. Specifically, pre- to post-operative changes in GAP, GT (hence RSA), LL (hence RLL) and UIV slope were associated with changes in compressive load, and almost all considered sagittal alignment measures correlated with changes in shear. In a subset of T10-pelvis fusion cases, postoperative GT, UIV slope, GAP and T10-L2 angles were associated with both postoperative compressive and shear loads. In other words, sagittal imbalance and malorientation of proximal vertebra after fusion were associated with greater compression and shear forces on the UIV level. Broader analyses of larger clinical samples should be performed in the future to unravel whether or not (or to what degree) spinal loads provide a causal mechanism explaining the previously reported association between sagittal alignment and mechanical complications.

Funding Study funding was provided by Maxi Foundation. Open access funding was provided by Swiss Federal Institute of Technology Zurich.

Declarations

Conflict of interest The authors declare that they have no conflict of interest.

Open Access This article is licensed under a Creative Commons Attribution 4.0 International License, which permits use, sharing, adaptation, distribution and reproduction in any medium or format, as long as you give appropriate credit to the original author(s) and the source, provide a link to the Creative Commons licence, and indicate if changes were made. The images or other third party material in this article are included in the article's Creative Commons licence, unless indicated otherwise in a credit line to the material. If material is not included in the article's Creative Commons licence and your intended use is not permitted by statutory regulation or exceeds the permitted use, you will need to obtain permission directly from the copyright holder. To view a copy of this licence, visit <http://creativecommons.org/licenses/by/4.0/>.

References


- Pellise F, Vila-Casademunt A, Ferrer M, Domingo-Sabat M, Bago J, Perez-Grueso FJ, Alanay A, Mannion AF, Acaroglu E, European Spine Study Group E (2015) Impact on health related quality of life of adult spinal deformity (ASD) compared with other chronic conditions. *Eur Spine J* 24:3–11. <https://doi.org/10.1007/s00586-014-3542-1>
- Diebo BG, Shah NV, Boachie-Adjei O, Zhu F, Rothenfluh DA, Paulino CB, Schwab FJ, Lafage V (2019) Adult spinal deformity. *The Lancet* 394:160–172. [https://doi.org/10.1016/s0140-6736\(19\)31125-0](https://doi.org/10.1016/s0140-6736(19)31125-0)
- United Nations (2020) World Population Ageing 2019. In., New York
- Youssef JA, Orndorff DO, Patty CA, Scott MA, Price HL, Hamlin LF, Williams TL, Uribe JS, Deviren V (2013) Current status of adult spinal deformity. *Global Spine J* 3:51–62. <https://doi.org/10.1055/s-0032-1326950>
- Bridwell KH, Glassman S, Horton W, Shaffrey C, Schwab F, Zebala LP, Lenke LG, Hilton JF, Shainline M, Baldus C, Wootton D (2009) Does treatment (nonoperative and operative) improve the two-year quality of life in patients with adult symptomatic lumbar scoliosis: a prospective multicenter evidence-based medicine study. *Spine* 34(20):2171–2178. <https://doi.org/10.1097/BRS.0b013e3181a8fde8>
- Sciubba DM, Yurter A, Smith JS, Kelly MP, Scheer JK, Goodwin CR, Lafage V, Hart RA, Bess S, Kebaish K, Schwab F, International Spine Study G (2015) A comprehensive review of complication rates after surgery for adult deformity: a reference for informed consent. *Spine Deform.* 3(6):575–594. <https://doi.org/10.1016/j.jspsd.2015.04.005>
- Kwan KYH, Lenke LG, Shaffrey CI, Carreon LY, Dahl BT, Fehlings MG, Ames CP, Boachie-Adjei O, Dekutoski MB, Kebaish KM, Lewis SJ, Matsuyama Y, Mehdian H, Qiu Y, Schwab FJ, Cheung KMC, Deformity AOSKF (2021) Are higher global alignment and proportion scores associated with increased risks of mechanical complications after adult spinal deformity surgery? An external validation. *Clin Orthop Relat Res* 479:312–320. <https://doi.org/10.1097/CORR.0000000000001521>
- Ham DW, Kim HJ, Choi JH, Park J, Lee J, Yeom JS (2021) Validity of the Global Alignment Proportion (GAP) score in predicting mechanical complications after adult spinal deformity surgery in elderly patients. *Eur Spine J.* <https://doi.org/10.1007/s00586-021-06734-2>

9. Yilgor C, Sogunmez N, Boissiere L, Yavuz Y, Obeid I, Kleinstuck F, Perez-Grueso FJS, Acaroglu E, Haddad S, Mannion AF, Pellice F, Alanay A, European Spine Study Group (2017) Global Alignment and Proportion (GAP) Score: Development and Validation of a New Method of Analyzing Spinopelvic Alignment to Predict Mechanical Complications After Adult Spinal Deformity Surgery. *J Bone Joint Surg Am* 99:1661–1672. <https://doi.org/10.2106/JBJS.16.01594>
10. Kawabata A, Yoshii T, Sakai K, Hirai T, Yuasa M, Inose H, Utagawa K, Hashimoto J, Matsukura Y, Tomori M, Torigoe I (2020) Identification of predictive factors for mechanical complications after adult spinal deformity surgery: a multi-institutional retrospective study. *Spine* 45(17):1185–1192. <https://doi.org/10.1097/BRS.0000000000003500>
11. Yagi M, Daimon K, Hosogane N, Okada E, Suzuki S, Tsuji O, Nagoshi N, Fujita N, Nakamura M, Matsumoto M, Watanabe K, Keio Spine Research G (2021) Predictive probability of the global alignment and proportion score for the development of mechanical failure following adult spinal deformity surgery in asian patients. *Spine* 46(2):E80–E86. <https://doi.org/10.1097/BRS.0000000000003738>
12. Bari TJ, Ohrt-Nissen S, Hansen LV, Dahl B, Gehrchen M (2019) Ability of the Global Alignment and Proportion score to predict mechanical failure following adult spinal deformity surgery—validation in 149 patients with two-year follow-up. *Spine Deform* 7:331–337. <https://doi.org/10.1016/j.jspd.2018.08.002>
13. Lau D, Clark AJ, Scheer JK, Daubs MD, Coe JD, Paonessa KJ, LaGrone MO, Kasten MD, Amaral RA, Trobisch PD, Lee JH, Committee SRSASD (2014) Proximal junctional kyphosis and failure after spinal deformity surgery: a systematic review of the literature as a background to classification development. *Spine* 39(25):2093–2102. <https://doi.org/10.1097/BRS.0000000000000627>
14. Schwab FJ, Hawkinson N, Lafage V, Smith JS, Hart R, Mundis G, Burton DC, Line B, Akbarnia B, Boachie-Adjei O, Hostin R, Shaffrey CI, Arlet V, Wood K, Gupta M, Bess S, Mummaneni PV, International Spine Study Group (2012) Risk factors for major peri-operative complications in adult spinal deformity surgery: a multi-center review of 953 consecutive patients. *Eur Spine J* 21:2603–2610. <https://doi.org/10.1007/s00586-012-2370-4>
15. Diebo BG, Henry J, Lafage V, Berjano P (2015) Sagittal deformities of the spine: factors influencing the outcomes and complications. *Eur Spine J* 24(Suppl 1):S3–15. <https://doi.org/10.1007/s00586-014-3653-8>
16. Hallager DW, Karstensen S, Bukhari N, Gehrchen M, Dahl B (2017) Radiographic predictors for mechanical failure after adult spinal deformity surgery: a retrospective cohort study in 138 patients. *Spine* 42(14):E855–E863. <https://doi.org/10.1097/BRS.0000000000001996>
17. Sebaaly A, Gehrchen M, Silvestre C, Kharrat K, Bari TJ, Kreichati G, Rizkallah M, Roussouly P (2020) Mechanical complications in adult spinal deformity and the effect of restoring the spinal shapes according to the Roussouly classification: a multicentric study. *Eur Spine J* 29:904–913. <https://doi.org/10.1007/s00586-019-06253-1>
18. Glassman SD, Berven S, Bridwell K, Horton W, Dimar JR (2005) Correlation of radiographic parameters and clinical symptoms in adult scoliosis. *Spine* (Phila Pa 1976) 30:682–688. <https://doi.org/10.1097/01.brs.0000155425.04536.f7>
19. Glassman SD, Bridwell K, Dimar JR, Horton W, Berven S, Schwab F (2005) The impact of positive sagittal balance in adult spinal deformity. *Spine* 30(18):2024–2029
20. Schwab FJ, Blondel B, Bess S, Hostin R, Shaffrey CI, Smith JS, Boachie-Adjei O, Burton DC, Akbarnia BA, Mundis GM, Ames CP, Kebaish K, Hart RA, Farcy JP, Lafage V, International Spine Study Group (2013) Radiographical spinopelvic parameters and disability in the setting of adult spinal deformity: a prospective multicenter analysis. *Spine* (Phila Pa 1976) 38:E803–812. <https://doi.org/10.1097/BRS.0b013e318292b7b9>
21. Jacobs E, van Royen BJ, van Kuijk SMJ, Merk JMR, Stadhouders A, van Rhijn LW, Willems PC (2019) Prediction of mechanical complications in adult spinal deformity surgery—the GAP score versus the Schwab classification. *Spine J* 19:781–788. <https://doi.org/10.1016/j.spinee.2018.11.013>
22. Ohba T, Ebata S, Oba H, Koyama K, Yokomichi H, Haro H (2019) Predictors of poor Global Alignment and Proportion score after surgery for adult spinal deformity. *Spine* (Phila Pa 1976) 44:E1136–E1143. <https://doi.org/10.1097/BRS.00000000000003086>
23. Noh SH, Ha Y, Obeid I, Park JY, Kuh SU, Chin DK, Kim KS, Cho YE, Lee HS, Kim KH (2020) Modified global alignment and proportion scoring with body mass index and bone mineral density (GAPB) for improving predictions of mechanical complications after adult spinal deformity surgery. *Spine J* 20:776–784. <https://doi.org/10.1016/j.spinee.2019.11.006>
24. Wang M, Xu L, Chen X, Zhou Q, Du C, Yang B, Zhu Z, Wang B, Qiu Y, Sun X (2021) Optimal reconstruction of sagittal alignment according to global alignment and proportion score can reduce adjacent segment degeneration after lumbar fusion. *Spine* (Phila Pa 1976) 46:E257–E266. <https://doi.org/10.1097/BRS.0000000000003761>
25. Keller TS, Colloca CJ, Harrison DE, Harrison DD, Janik TJ (2005) Influence of spine morphology on intervertebral disc loads and stresses in asymptomatic adults: implications for the ideal spine. *Spine J* 5:297–309. <https://doi.org/10.1016/j.spinee.2004.10.050>
26. Shirazi-Adl A, El-Rich M, Pop DG, Parnianpour M (2005) Spinal muscle forces, internal loads and stability in standing under various postures and loads—application of kinematics-based algorithm. *Eur Spine J* 14:381–392. <https://doi.org/10.1007/s00586-004-0779-0>
27. Briggs AM, Wrigley TV, van Dieen JH, Phillips B, Lo SK, Greig AM, Bennell KL (2006) The effect of osteoporotic vertebral fracture on predicted spinal loads in vivo. *Eur Spine J* 15:1785–1795. <https://doi.org/10.1007/s00586-006-0158-0>
28. Briggs AM, van Dieen JH, Wrigley TV, Greig AM, Phillips B, Lo SK, Bennell KL (2007) Thoracic kyphosis affects spinal loads and trunk muscle force. *Phys Ther* 87:595–607. <https://doi.org/10.2522/ptj.20060119>
29. Bruno AG, Anderson DE, D’Agostino J, Bouxsein ML (2012) The effect of thoracic kyphosis and sagittal plane alignment on vertebral compressive loading. *J Bone Miner Res* 27:2144–2151. <https://doi.org/10.1002/jbmr.1658>
30. Bruno AG, Burkhart K, Allaire B, Anderson DE, Bouxsein ML (2017) Spinal loading patterns from biomechanical modeling explain the high incidence of vertebral fractures in the thoracolumbar region. *J Bone Miner Res* 32:1282–1290. <https://doi.org/10.1002/jbmr.3113>
31. Roussouly P, Golloly S, Berthonnaud E, Dimnet J (2005) Classification of the normal variation in the sagittal alignment of the human lumbar spine and pelvis in the standing position. *Spine* (Phila Pa 1976) 30:346–353. <https://doi.org/10.1097/01.brs.0000152379.54463.65>
32. Bassani T, Casaroli G, Galbusera F (2019) Dependence of lumbar loads on spinopelvic sagittal alignment: an evaluation based on musculoskeletal modeling. *PLoS ONE* 14:e0207997. <https://doi.org/10.1371/journal.pone.0207997>
33. Senteler M, Weisse B, Snedeker JG, Rothenfluh DA (2014) Pelvic incidence–lumbar lordosis mismatch results in increased segmental joint loads in the unfused and fused lumbar spine. *Eur Spine J* 23:1384–1393. <https://doi.org/10.1007/s00586-013-3132-7>
34. Senteler M, Weisse B, Rothenfluh DA, Farshad MT, Snedeker JG (2017) Fusion angle affects intervertebral adjacent spinal segment

- joint forces-Model-based analysis of patient specific alignment. *J Orthop Res* 35:131–139. <https://doi.org/10.1002/jor.23357>
35. Ignasiak D, Dendorfer S, Ferguson SJ (2016) Thoracolumbar spine model with articulated ribcage for the prediction of dynamic spinal loading. *J Biomech* 49:959–966. <https://doi.org/10.1016/j.jbiomech.2015.10.010>
 36. Ignasiak D, Ferguson SJ, Arjmand N (2016) A rigid thorax assumption affects model loading predictions at the upper but not lower lumbar levels. *J Biomech* 49:3074–3078. <https://doi.org/10.1016/j.jbiomech.2016.07.006>
 37. de Zee M, Hansen L, Wong C, Rasmussen J, Simonsen EB (2007) A generic detailed rigid-body lumbar spine model. *J Biomech* 40:1219–1227. <https://doi.org/10.1016/j.jbiomech.2006.05.030>
 38. Bassani T, Stucovitz E, Qian Z, Briguglio M, Galbusera F (2017) Validation of the AnyBody full body musculoskeletal model in computing lumbar spine loads at L4L5 level. *J Biomech* 58:89–96. <https://doi.org/10.1016/j.jbiomech.2017.04.025>
 39. Ignasiak D, Peteler T, Fekete TF, Haschtmann D, Ferguson SJ (2018) The influence of spinal fusion length on proximal junction biomechanics: a parametric computational study. *Eur Spine J* 27:2262–2271. <https://doi.org/10.1007/s00586-018-5700-3>
 40. Damsgaard M, Rasmussen J, Christensen ST, Surma E, de Zee M (2006) Analysis of musculoskeletal systems in the AnyBody Modeling System. *Simul Model Pract Theory* 14:1100–1111. <https://doi.org/10.1016/j.simpat.2006.09.001>
 41. Erdemir A, McLean S, Herzog W, van den Bogert AJ (2007) Model-based estimation of muscle forces exerted during movements. *Clin Biomech Bristol Avon* 22:131–154. <https://doi.org/10.1016/j.clinbiomech.2006.09.005>
 42. Rasmussen J, Damsgaard M, Voigt M (2001) Muscle recruitment by the min/max criterion—a comparative numerical study. *J Biomech* 34:409–415
 43. Magerl F, Aebi M, Gertzbein SD, Harms J, Nazarian S (1994) A comprehensive classification of thoracic and lumbar injuries. *Eur Spine J* 3:184–201
 44. Le Huec JC, Richards J, Tsoupras A, Price R, Leglise A, Faundez AA (2018) The mechanism in junctional failure of thoraco-lumbar fusions. Part I: Biomechanical analysis of mechanisms responsible of vertebral overstress and description of the cervical inclination angle (CIA). *Eur Spine J* 27:129–138. <https://doi.org/10.1007/s00586-017-5425-8>
 45. Gallagher S, Marras WS, Litsky AS, Burr D (2006) An exploratory study of loading and morphometric factors associated with specific failure modes in fatigue testing of lumbar motion segments. *Clin Biomech Bristol Avon* 21:228–234. <https://doi.org/10.1016/j.clinbiomech.2005.10.001>
 46. Buell TJ, Chen CJ, Quinn JC, Buchholz AL, Mazur MD, Mullin JP, Nguyen JH, Taylor DG, Bess S, Line BG, Ames CP, Schwab FJ, Lafage V, Shaffrey CI, Smith JS (2019) Alignment risk factors for proximal junctional kyphosis and the effect of lower thoracic junctional tethers for adult spinal deformity. *World Neurosurg* 121:e96–e103. <https://doi.org/10.1016/j.wneu.2018.08.242>
 47. Nicholls FH, Bae J, Theologis AA, Eksi MS, Ames CP, Berven SH, Burch S, Tay BK, Deviren V (2017) Factors associated with the development of and revision for proximal junctional kyphosis in 440 consecutive adult spinal deformity patients. *Spine (Phila Pa 1976)* 42:1693–1698. <https://doi.org/10.1097/BRS.0000000000002209>
 48. Aquarius R, Homminga J, Verdonschot N, Tanck E (2011) The fracture risk of adjacent vertebrae is increased by the changed loading direction after a wedge fracture. *Spine (Phila Pa 1976)* 36:E408–412. <https://doi.org/10.1097/BRS.0b013e3181f0f726>
 49. Lafage R, Line BG, Gupta S, Liabaud B, Schwab F, Smith JS, Gum JL, Ames CP, Hostin R, Mundis GM Jr, Kim HJ, Bess S, Klineberg E, Lafage V, International Spine Study Group (2017) Orientation of the upper-most instrumented segment influences proximal junctional disease following adult spinal deformity surgery. *Spine (Phila Pa 1976)* 42:1570–1577. <https://doi.org/10.1097/BRS.0000000000002191>
 50. Yagi M, King AB, Boachie-Adjei O (2012) Incidence, risk factors, and natural course of proximal junctional kyphosis: surgical outcomes review of adult idiopathic scoliosis. Minimum 5 years of follow-up. *Spine (Phila Pa 1976)* 37:1479–1489. <https://doi.org/10.1097/BRS.0b013e31824e4888>
 51. Kim DK, Kim JY, Kim DY, Rhim SC, Yoon SH (2017) Risk factors of proximal junctional kyphosis after multilevel fusion surgery: more than 2 years follow-up data. *J Korean Neurosurg Soc* 60:174–180. <https://doi.org/10.3340/jkns.2016.0707.014>
 52. Inoue S, Khashan M, Fujimori T, Berven SH (2015) Analysis of mechanical failure associated with reoperation in spinal fusion to the sacrum in adult spinal deformity. *J Orthop Sci* 20:609–616. <https://doi.org/10.1007/s00776-015-0729-1>
 53. Wang T, Ding W (2020) Risk factors for adjacent segment degeneration after posterior lumbar fusion surgery in treatment for degenerative lumbar disorders: a meta-analysis. *J Orthop Surg Res* 15:582. <https://doi.org/10.1186/s13018-020-02032-7>
 54. Yagi M, Hosogane N, Watanabe K, Asazuma T, Matsumoto M, Keio Spine Research Group (2016) The paravertebral muscle and psoas for the maintenance of global spinal alignment in patient with degenerative lumbar scoliosis. *Spine J* 16:451–458. <https://doi.org/10.1016/j.spinee.2015.07.001>
 55. Katsu M, Ohba T, Ebata S, Oba H, Koyama K, Haro H (2020) Potential role of paraspinal musculature in the maintenance of spinopelvic alignment in patients with adult spinal deformities. *Clin Spine Surg* 33:E76–E80. <https://doi.org/10.1097/BSD.0000000000000862>
 56. Ignasiak D, Valenzuela W, Reyes M, Ferguson SJ (2018) The effect of muscle ageing and sarcopenia on spinal segmental loads. *Eur Spine J* 27:2650–2659. <https://doi.org/10.1007/s00586-018-5729-3>
 57. Malakoutian M, Street J, Wilke HJ, Stavness I, Dvorak M, Fels S, Oxland T (2016) Role of muscle damage on loading at the level adjacent to a lumbar spine fusion: a biomechanical analysis. *Eur Spine J* 25:2929–2937. <https://doi.org/10.1007/s00586-016-4686-y>
 58. Roussouly P, Pinheiro-Franco JL (2011) Biomechanical analysis of the spino-pelvic organization and adaptation in pathology. *Eur Spine J* 20(Suppl 5):609–618. <https://doi.org/10.1007/s00586-011-1928-x>
 59. Roussouly P, Nnadi C (2010) Sagittal plane deformity: an overview of interpretation and management. *Eur Spine J* 19:1824–1836. <https://doi.org/10.1007/s00586-010-1476-9>
 60. Barrey C, Roussouly P, Le Huec JC, D’Acunzi G, Perrin G (2013) Compensatory mechanisms contributing to keep the sagittal balance of the spine. *Eur Spine J* 22(Suppl 6):S834–841. <https://doi.org/10.1007/s00586-013-3030-z>

Publisher's Note Springer Nature remains neutral with regard to jurisdictional claims in published maps and institutional affiliations.

Authors and Affiliations

Dominika Ignasiak¹  · Pascal Behm¹ · Anne F. Mannion² · Fabio Galbusera² · Frank Kleinstück³ · Tamás F. Fekete³ · Daniel Haschtmann³ · Dezső Jézenszky³ · Laura Zimmermann² · Sarah Richner-Wunderlin² · Alba Vila-Casademunt⁴ · Ferran Pellisé⁵ · Ibrahim Obeid⁶ · Javier Pizones⁷ · Francisco J. Sánchez Pérez-Grueso⁷ · Muhammed Ilkay Karaman⁸ · Ahmet Alanay⁹ · Çağlar Yilgor⁹ · Stephen J. Ferguson¹ · Markus Loibl³ · ESSG European Spine Study Group

¹ Institute for Biomechanics, ETH Zurich, HPP O13, Hönggerberggring 64, 8093 Zurich, Switzerland

² Department of Teaching, Research and Development, Schulthess Klinik, Zurich, Switzerland

³ Department of Spine Surgery, Schulthess Klinik, Zurich, Switzerland

⁴ Spine Research Unit, Vall d'Hebron Institute of Research, Barcelona, Spain

⁵ Spine Surgery Unit, Hospital Vall d'Hebron, Barcelona, Spain

⁶ Pellegrin Bordeaux University Hospital, 33000 Bordeaux, France

⁷ Spine Surgery Unit, Hospital Universitario La Paz, Madrid, Spain

⁸ Acibadem Mehmet Ali Aydınlar University School of Medicine, Istanbul, Turkey

⁹ Department of Orthopedics and Traumatology, Acibadem Mehmet Ali Aydınlar University School of Medicine, Istanbul, Turkey